RSC Advances

ROYAL SOCIETY OF CHEMISTRY

www.rsc.org/advances

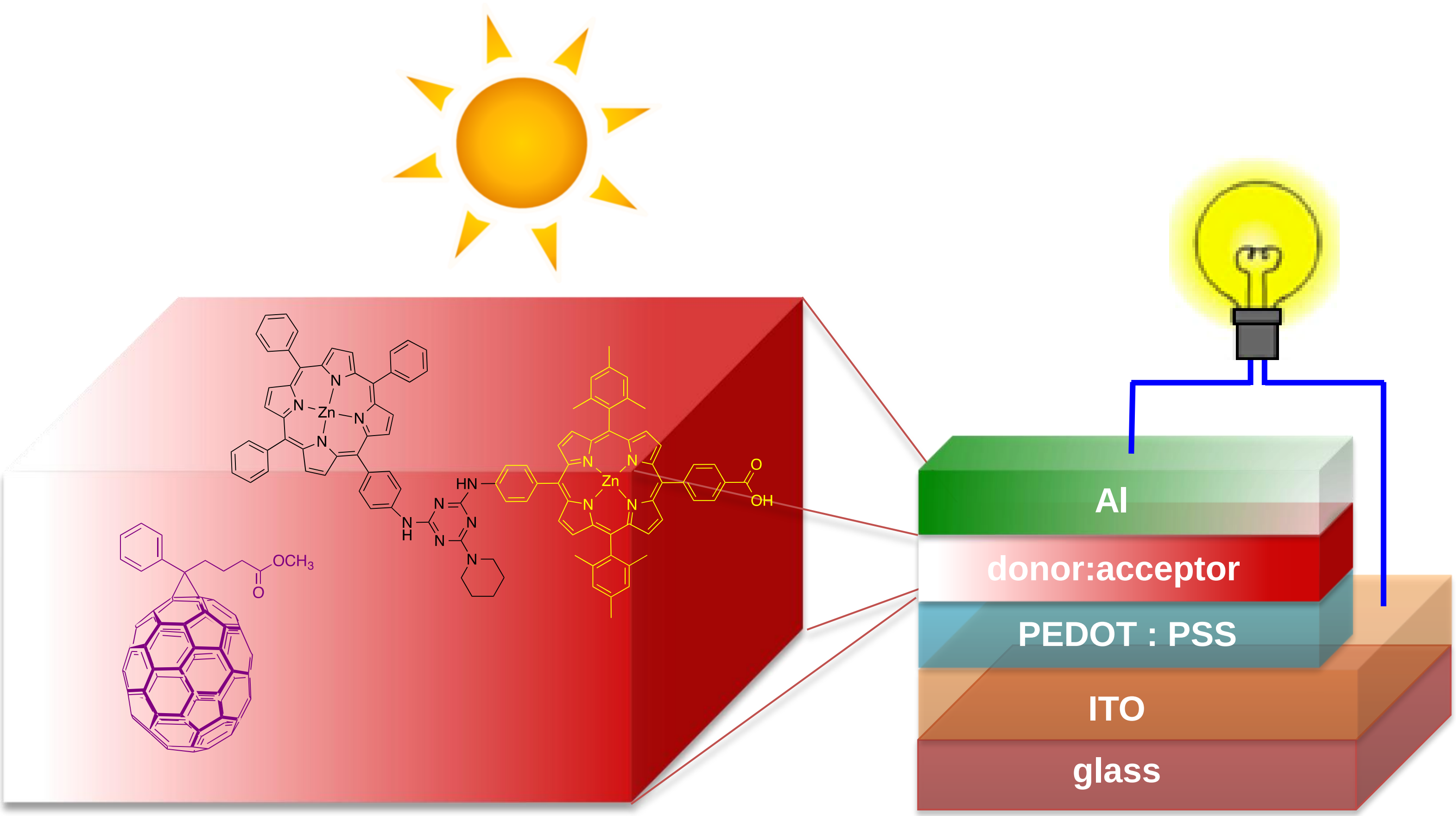
Zn
N
HN
N
H
OCH3
O
OH
Al
donor:acceptor
PEDOT : PSS
ITO
glass

New solution processed bulk-heterojunction organic solar cells based on a triazine-bridged porphyrin dyad as electron donor

Ganesh D. Sharma[1]*,*Galateia E. Zervaki*[2], *Panagiotis Angaridis*[3], *and Athanassios G. Coutsolelos*[3]*

[1]R&D Centre for Engineering and Science, JEC Group of Colleges, Jaipur Engineering
College Campus, Kukas, Jaipur, Raj 303101, India

[2]Department of Chemistry, University of Crete, Laboratory of Bioinorganic Chemistry,
Voutes Campus, P.O. Box 2208, 71003 Heraklion, Crete, Greece

[3]Department of Chemistry, Aristotle University of Thessaloniki, Thessaloniki, 54124, Greece

Keywords: BHJ solar cells, $PC_{71}BM$, porphyrin dyad, triazine, piperidine

*Corresponding Authors

E-mail: coutsole@chemistry.uoc.gr (A.G.C.); gdsharma273@gmail.com (G.D.S.).

Abstract

An unsymmetrical porphyrin dyad (ZnP)-[triazine-*N*pip]-(ZnPCOOH) or P-t*N*p-P′ consisted of two zinc-metallated porphyrin units covalently linked through their peripheral aryl-amino groups to a central triazine group, to which an *N*-piperidine group is also attached, has been used in combination with $PC_{71}BM$ ([6,6]-phenyl C71 butyric acid methyl ester) as electron donor and acceptor, respectively, for the active layer of solution-processed bulk hetero-junction (BHJ) organic solar cells. The photophysical properties of P-t*N*p-P′ and $PC_{71}BM$ blend films, as well as cyclic voltammetry measurements of the porphyrin dyad, suggest that P-t*N*p-P′ can effectively harvest photons and transfer electrons to $PC_{71}BM$. The BHJ organic solar cell based on the P-t*N*p-P′:$PC_{71}BM$ active layer blend in 1:1 weight ratio processed from THF resulted in a power conversion efficiency (PCE) of 2.91%. A significant improvement of the overall photovoltaic efficiency was achieved up to 4.16% when the active layer blend was processed from a 3% v/v mixture of pyridine in THF. This was ascribed to an enhancement of the short circuit current J_{sc} of the solar cell, which is related to the different surface morphology of the P-t*N*p-P′:$PC_{71}BM$ active layer blend upon addition of pyridine. The pyridine-modified active layer exhibits a higher degree of crystallinity, as confirmed by the X-ray diffraction pattern and AFM images of the corresponding film, which results in an increase of exciton dissociation efficiency and more balanced charge transport.

Introduction

Organic solar cells are light-weight and large-area devices which are based on inexpensive, flexible, semi-conducting organic materials. Owing to their attractive properties, compared to the conventional inorganic solar cells, they appear to be a very interesting and promising technology considered part of next generation photovoltaic devices.[1-5] To date, the most efficient type of organic solar cell devices is solution-processed bulk hetero-junction (BHJ) organic solar cells. They consist of an active layer blend of a photoactive, conjugated polymer material acting as electron-donor, and a functionalized fullerene molecule acting as electron-acceptor,[1, 6-8] sandwiched between two electrodes. The photoactive polymer absorbs photons and creates electron-hole pairs (excitons), which diffuse into the donor/acceptor interfaces, and, finally, separate into electrons and holes which travel to the corresponding electrodes producing electric current. By using appropriately designed conjugated, polymeric, photo-active materials, and controlling the morphology of the active layer, solar cells with power conversion efficiencies (PCE) that exceed 9% have been reported.[9-13] However, despite their success, conjugated polymers pose some problems related to the reproducibility of their synthesis, purification and, hence, their electronic properties. In addition, crude materials contain various chain lengths and require fractioning with different solvents in order to reduce polydispersity. Furthermore, it is generally necessary to remove remnant terminal groups by appropriate chemical treatment. These additional processes increase the cost and environmental impact of the material.

The use of appropriate small molecules instead of conjugated polymers as photoactive electron donors in the active layer has recently been the focus of many research efforts on solution-processed BHJ solar cells, since they offer many advantages over their polymer counterparts, including well-defined molecular structure and molecular weight, high purity and good batch-to-batch reproducibility.[14-18] Research work in this area was initiated in 2005 and it has been rapidly progressed.[18, 19-22] In particular, π-conjugated molecules with a donor-acceptor (D-A) molecular structure have been very successful, due to their potential to create very efficient electron-hole separation, and they have resulted in BHJ solar cells with PCE values as high as those obtained with the most successful conjugated polymers,[19]or even higher, after device optimization.[23,24] Remarkably, there has been a recent report with a record breaking 12% solar cell efficiency,[25] demonstrating the high potential of solution-processed small molecule BHJ solar cells over polymer donors.

Donor molecules employed in the active layers of BHJ solar cells, due to their significant role in absorbing and harvesting solar radiation, should display a strong and wide absorption profile. Furthermore, they should be sufficiently soluble in common solvents, be able to exhibit strong intermolecular interactions in the solid state, have conduction band edge that is higher than that of the acceptor material, and exhibit high stability towards light and air.

Inspired by photosynthesis, which incorporates porphyrin-type macrocycles as basic chromophore units for harvesting solar energy and converting it to chemical energy through a series of photoinduced electron and energy transfer processes, porphyrins appear to be very attractive as donor molecules in BHJ solar cells. Due to their conjugated macrocyclic framework, they display a strong Soret band at 400-450 nm and moderate Q-bands in the 550-650 nm region of their absorption spectra, [26] while by appropriate modification of the substitutents on the macrocyclic ring allows fine tuning of their electronic, spectroscopic and physical properties. Interestingly, despite their wide and successful utilization of porphyrins in other types of solar cells, e.g. in dye-sensitized solar cells (DSSCs), [27-31] which have resulted in devices with PCE values higher than 13%, [32,33] their use in BHJ solar cells has been rather limited, [34-38] However, recent results suggest that porphyrins can be very effective as electron donors in small molecule BHJ organic solar cells and their performance can be significantly enhanced via suitable molecular design. For example, in 2012, it was reported that the use of a *meso*-tetraethynyl substituted porphyrin with terminal aromatic and aliphatic groups was used as electron donor, in combination with $PC_{60}BM$ ([6,6]-phenyl C_{60} butyric acid methyl ester) as electron acceptor, resulted in a BHJ solar cell which resulted in a PCE value of 2.5%.[39] In another case, a porphyrin with two benzothiadiazole units, end-caped with 3-hexylthienyl, which are connected to opposite *meso* positions of the porphyrin core by ethynyl bridges, in combination with [6,6]-phenyl C_{71} butyric acid methyl ester ($PC_{71}BM$), resulted a solar cell with a PCE value of 4.02%. [40] By utilizing a porphyrin donor with two diketopyrrolopyrrole units and ethynyl bridges with bulky substituents at *meso* positions and $PC_{60}BM$, a solar cell with a PCE value of 3.71% was obtained, which was improved to 4.78% by incorporating pyridine into the active layer.[41] More recently, the use of an analogous porphyrin derivative with two diketopyrrolopyrrole units with less bulky substituents at the periphery as donor along with $PC_{61}BM$ as acceptor raised PCE up to 7.23%. [42] We recently reported a simple porphyrin derivative with an ethynyl pyridinyl group at a *meso*- position, which was used in combination with $PC_{71}BM$, achieving a PCE value of 2.54% without any additive. [43]

Over the course of our studies on the synthesis and utilization of new porphyrins and porphyrin assemblies in solar cell applications,[44] we have synthesized a variety of novel triazine-based porphyrin assemblies and investigated their utilization in solar cell applications, as sensitizers in DSSCs[45,46] and as electron donors in BHJ solar cells.[43,47] In general, triazine derivatives have been extensively studied as electron transporting and hole blocking layers.[48-52] On the other hand, porphyrin units covalently linked through electron deficient π-conjugated groups like triazine are known to be *p*-type semiconductors.[34,38,53,54] Therefore, such kind of assemblies is expected to be functional as electron donors in BHJ solar cells and possibly offer the advantage of enhanced charge extraction efficiency.[55] Along these lines, we recently reported a triazine-bridged porphyrin triad with the 2D-π-A molecular architecture[56], which in combination with $PC_{71}BM$ resulted in a BHJ solar cell with a PCE value of 2.85 and 3.93% without and with 1-chloronaphathalene (CN) additive.[47]

Herein we report the use of an unsymmetrical triazine-bridged porphyrin dyad P-t*N*p-P′ (Scheme 1), which consists of two *meso*- aryl-substituted zinc metallated porphyrin units and a piperidine group (with the D-A-D molecular architecture), blended together with $PC_{71}BM$ (Scheme 2), as electron donor and electron acceptor, respectively, for the photoactive layer of solution processed small molecule BHJ solar cells. By using a P-t*N*p-P′:$PC_{71}BM$ active layer blend in 1:1 weight ratio processed form THF an overall PCE value of 2.91% was obtained. The efficiency of the solar cell was further enhanced up to 4.16% when the active layer blend was processed from 3% v/v mixture of pyridine in THF.

Experimental details

General methods and materials. All synthetic manipulations were carried out using standard Schlenk techniques under nitrogen atmosphere. 2,4,6-Trichloro-1,3,5-triazine (cyanuric chloride), diisopropylethylamine (DIPEA), $Zn(CH_3COO)_2{\cdot}2H_2O$, KOH, $PC_{71}BM$, pyridine and other chemicals and solvents were purchased from usual commercial sources and used as received, unless otherwise stated. Tetrahydrofuran (THF) was freshly distilled from Na/benzophenone.5-(4-Carbomethoxyphenyl)-15-(4-aminophenyl)-10,20-bis(2,4,6-trimethylphenyl)-porphyrin and 5-(4-aminophenyl)-10,15,20-triphenyl-porphyrin were prepared according to literature procedures.[46,57]

Synthesis of porphyrindyad P-t*N*p-P′. P-t*N*p-P′ was prepared by adding consecutively to a THF solution of cyanuric chloride, in the presence of excess of DIPEA, one equivalent of 5-(4-carbomethoxyphenyl)-15-(4-aminophenyl)-10,20-bis(2,4,6-trimethylphenyl)-porphyrin) at low temperature, an excess of 5-(4-aminophenyl)-10,15,20-triphenyl-porphyrin at room temperature and an excess of piperidine at elevated temperature (~65^{o}C), followed by zincmetallation with $Zn(CH_3COO)_2{\cdot}2H_2O$ and basic hydrolysis with KOH. Satisfactory analytical and spectroscopic characteristics were obtained and reported in our earlier communication.[46]

Photophysical measurements. UV-vis absorption spectra were measured on a Shimadzu UV-1700 spectrophotometer using 10 mm path-length cuvettes. Photoluminescence spectra were measured on a JASCO FP-6500 fluorescence spectrophotometer equipped with a red sensitive WRE-343 photomultiplier tube.

Electrochemistry measurements. Cyclic voltammetry experiments were carried out at room temperature using an AutoLab PGSTAT20 potentiostat and appropriate routines available in the operating software (GPES, version 4.9). Measurements were carried out in freshly distilled and deoxygenated CH_2Cl_2, at a rate of 100 mV/s with a solute concentration of 1.0 mM in the presence of tetrabutylammoniumhexafluorophosphate (0.1 M) as supporting electrolyte. A three-electrode cell setup was used with a platinum working electrode, a saturated calomel (SCE) reference electrode, and a platinum wire as counter electrode.

X-ray powder diffraction (XRD) measurements. XRD measurements were recorded on a Bruker D8 Advanced model diffractometer with Cu Kα radiation (λ = 1.542 Å) at a generator voltage of 40 kV.

Solar cell fabrication. The BHJ organic solar cells were fabricated using the glass/ITO/PEDOT:PSS/P-t*N*p-P′:$PC_{71}BM$/Al device architecture. The indium tin oxide (ITO) patterned substrates were cleaned by ultrasonic treatment in aqueous detergent, deionized water, isopropyl alcohol, and acetone sequentially, and finally dried under ambient conditions. The anode consisted of glass substrates pre-coated with ITO, modified by spin coating with a PEDOT:PSS layer (60 nm) as hole transport and heated for 10 min at 100°C. Mixtures of P-t*N*p-P′ and $PC_{71}BM$ with weight ratios of 1:05, 1:1, and 1:1.5 in THF were prepared and spin-cast onto the PEDOT:PSS layer and dried overnight at ambient atmosphere. For the P-t*N*p-P′:$PC_{71}BM$ blend, processed from 3% v/v of pyridine in THF solvent mixture only the 1:1 weight ratio was used. The thickness of the active layers was ~90 nm. The aluminum (Al) top electrode was thermally deposited on the active layer at a vacuum of 10^{-5} Torr through a shadow mask of area of 0.20 cm^2. All devices were fabricated and tested in ambient atmosphere without encapsulation. In order to measure the hole and electron mobility of the solar cells, the hole-only and electron-only devices with ITO/PEODT:PSS/P-t*N*p-P′:$PC_{71}BM$/Au and Al/P-t*N*p-P′:$PC_{71}BM$/Al architectures, respectively, were also fabricated in an analogous way.

Photovoltaic measurements. The current-voltage characteristics of the BHJ organic solar cells were measured using a computer controlled Keithley 238 source meter in dark as well as under simulated AM1.5G illumination of 100 mW/cm^2. A xenon light source coupled with optical filter was used to give the stimulated irradiance at the surface of the devices. The incident photon to current efficiency (IPCE) of the devices was measured, illuminating the device through the light source and monochromator and the resulting current was measured using a Keithley electrometer under short circuit condition.

Results and Discussion

Structure and synthesis of porphyrindyad P-t*N*p-P′.Porphyrin dyad P-t*N*p-P′ (Scheme 1) consists of two *meso* aryl-substituted zinc-metallated porphyrin units, one of which contains a terminal carboxylic acid group (i.e. 5-(4-aminophenyl)-10,15,20-triphenyl-porphyrin zinc and 5-(4-carboxyphenyl)-15-(4-aminophenyl)-10,20-bis(2,4,6-trimethylphenyl)-porphyrin zinc), which are covalently linked through their peripheral aryl-amino groups to a central s-triazine moiety. A N-substituted piperidine group further functionalizes the triazine ring. Therefore, P-t*N*p-P′ is an unsymmetrical dyad whose structure can be described as having the D-A-D molecular architecture.

P-t*N*p-P′ was synthesized via temperature-dependent, stepwise amination reactions of cyanuric chloride, which is the precursor of *s*-triazine, with two different amino-phenyl porphyrins, and piperidine, in the presence of a weak base (DIPEA). [46]

Photophysical properties of porphyrin dyad P-t*N*p-P′. The UV-vis absorption spectra of P-t*N*p-P′ in solution and in thin film are shown in Figure1. Its solution spectrum in THF (Figure 1, black-color line) exhibits the characteristic absorption bands of zinc-metallated porphyrin macrocycles, with an intense Soret band at 425 nm and two moderate Q bands at 557 and 597 nm, with molar extinction coefficients of 6.66×10^5, 0.28×10^5, and 0.12×10^5 M^{-1} cm^{-1} at 425, 557, and 597 nm, respectively, and no other additional features. This is an indication of negligible intramolecular communication between the individual porphyrin units attached to the triazine ring in the ground state of the dyad. The absorption spectrum of P-t*N*p-P′ in thin film form cast from THF (Figure 1, red-color line) exhibits the same absorption bands which are broader and slightly red-shifted than those of the solution spectrum. This may be attributed to porphyrin aggregation in solid state. By using the onset absorption edge λ_{onset} of Q bands on thin film and the expression $E_g^{opt} = 1240/\lambda_{onset}$, the optical band gap of P-t*N*p-P′ was calculated to be 1.94 eV.

In order to investigate the ability of P-t*N*p-P′ to serve as electron donor in the BHJ active layer of a solar cell, together with $PC_{71}BM$ as electron acceptor, the photoluminescence spectra of P-t*N*p-P′ and P-t*N*p-P′:$PC_{71}BM$ blend (in 1:1 ratio) were recorded. The photoluminescence spectrum of P-t*N*p-P′ in THF solution, upon excitation at its absorption maximum of the Soret band (425 nm), exhibits two peaks of unequal intensities at 608 and 657 nm (Figure 2, black-color line). When adsorbed onto thin film, the two emission peaks of P-t*N*p-P′ appear to be broader than those of the solution spectrum, while the lower intensity peak at 648 nm is slightly blue-shifted (Figure 2, red-color line), which is attributed to aggregation phenomena. However, when the P-t*N*p-P′:$PC_{71}BM$ (1:1 ratio) blend adsorbed onto thin film is photoexcited at 425 nm, the P-t*N*p-P′ emission is almost completely quenched (Figure 2, blue-color line). This is an indication of electron or energy transfer taking place from the porphyrin dyad P-t*N*p-P′ (electron donor) to $PC_{71}BM$ (electron acceptor). Consequently, the P-t*N*p-P′:$PC_{71}BM$ (1:1 ratio) blend can effectively be used as photoactive layer in BHJ organic solar cells for efficient light harvesting of solar energy that can facilitate exciton dissociation and photoinduced charge transfer.[42, 58-60]

Electrochemical properties of porphyrin dyad P-t*N*p-P′. The electrochemical properties of the porphyrin dyad P-t*N*p-P′ were investigated by cyclic voltammetry measurements in THF and revealed one oxidation process at $E_{ox}^{1} = +0.98$ V and one reduction processes at $E_{red}^{1} = -1.40$ *vs* SCE. Based on the first oxidation potential (E_{ox}^{1}) and the first reduction potential (E_{red}^{1}) of P-t*N*p-P′, the highest-occupied molecular orbital (HOMO) and lowest-occupied molecular orbital (LUMO) energy levels of P-t*N*p-P′ were estimated according to the expressions

$$E_{HOMO} = - (E^{ox} + 4.71) \text{ eV}$$

$$E_{LUMO} = - (E^{red} + 4.71) \text{ eV}$$

and they were found to be -5.69 eV and -3.31 eV, respectively. Taking into account that the HOMO and LUMO energy levels of $PC_{71}BM$ are -6.2 and -4.0 eV, respectively, the differences between the HOMO and LUMO energy levels of P-t*N*p-P′ and $PC_{71}BM$ are found to be 0.51 and 0.69 eV, respectively. This is an indication that there is sufficient driving force for efficient photo-induced electron-hole dissociation in the active layer of P-t*N*p-P′:$PC_{71}BM$.

Photovoltaic properties of P-t*N*p-P′:PC_{71}BM based BHJ organic solar cells. In general, the photovoltaic performance of BHJ solar cells depend on the relative amounts of the electron donor and electron acceptor materials used in the photoactive layer. For this reason, solar cells based on the general device structure glass/ITO//PEDOT:PSS/P-t*N*p-P′:$PC_{71}BM$/Al were fabricated using four different active layers consisted of mixtures of P-t*N*p-P′ and $PC_{71}BM$ blended in THF in different weight ratios, i.e. 1:0.5, 1:1, 1:1.5, and 1:2. The optimum device performance was found for the 1:1 weight ratio.

The current-voltage (J-V) characteristics of the BHJ solar cell with the P-t*N*p-P′:$PC_{71}BM$active layer blend in 1:1 weight ratio processed from THF are depicted in Figure 3a (black-color line), while the corresponding photovoltaic cell parameters, i.e. short circuit current (J_{sc}), open circuit voltage (V_{oc}) and fill factor (FF) are summarized in Table 1. The device exhibits J_{sc} =6.75 mA/cm^2, V_{oc} = 0.98 V and FF=0.44, resulting in an overall PCE value of 2.91%.

The IPCE response of the aforementioned BHJ organic solar cell was estimated from the expression

$$IPCE\ (\lambda) = 1240\ J_{sc}/\lambda P_{in}$$

where J_{sc} is the photocurrent under short circuit condition, λ is the wavelength of the incident monochromatic light and P_{in} is the incident photon flux. The IPCE spectrum of the device (shown in Figure 3b, black-color line) resembles the UV-vis absorption spectrum of the P-t*N*p-P′:$PC_{71}BM$ thin film, which indicates that P-t*N*p-P′ and $PC_{71}BM$ form an efficient active layer in which both of them contribute to the photocurrent generation.

There are only a few examples in the literature in which covalently linked porphyrin assemblies are used as electron donors in BHJ organic solar cells. The first assembly of this type to be reported, a symmetrical, triazine-linked, zinc-metallated porphyrin triad, resulted in a very poor photovoltaic performance (a PCE value of 0.5%).[55] More recently we reported a BHJ solar cell based on an unsymmetrical triazine-linked porphyrin triad as electron donor. The 2D-π-A structure architecture of that triad assisted in more efficient intramolecular charge transfer than the symmetrical triad, leading to a higher PCE value of 2.85% without any additive.[47]

The use of the unsymmetrical, triazine-based porphyrin dyad P-t*N*p-P′, with the D-A-D molecular architecture as donor in BHJ solar cells presented herein results in a similar PCE value (2.91%) which, however, considering the latest developments on polymer and small molecule based BHJ organic solar cell devices, is considered to be poor. Clearly, this may be ascribed to the low photovoltaic parameters of the solar cell. Interestingly, the V_{oc} value appears to be relatively high, which may be attributed to the low HOMO energy level of P-t*N*p-P′, since the V_{oc} is directly related to the difference between the LUMO energy level of the acceptor and HOMO energy level of the donor components employed in the BHJ active layer. Therefore, the reason for the poor photovoltaic performance should be due to the low J_{sc}, and *FF* values of the solar cell. These parameters are related to the light harvesting efficiency of the BHJ active layer, film morphology, charge transport, and charge collection on the respective electrodes of the solar cell.

The morphology of the active layer of a BHJ solar cell is of great importance for the photovoltaic parameters and the solar cell efficiency, since it significantly affects the charge transfer process. For this reason, many attempts have been focused on the improvement of its properties by means of various treatment methodologies, which include thermal annealing,[61,62] solvent annealing,[2, 63-65] and solvent additives.[66-71]

In an effort to improve the overall performance of the BHJ organic solar cell based on the P-t*N*p-P′:$PC_{71}BM$ active layer blend in 1:1 weight ratio, the solvent additive method was used. In particular, the active layer was processed from THF using pyridine as solvent additive, in a variety of different concentrations, i.e. 1, 2, 3, and 4% v/v pyridine in THF. The optimum concentration that resulted in the maximum PCE value was found to be 3% v/v.

The current-voltage (*J-V*) characteristics of the modified solar cell with the active layer prepared from a 3% v/v pyridine/THF mixture are shown in Figure 3a (red-color line), and the corresponding photovoltaic parameters are listed in Table 1.Remarkably, the latter solar cell displays an enhanced performance, since both J_{sc} (= 8.52 mA/cm^2) and FF (= 0.52) values are improved, and, despite the fact that V_{oc} is slightly lower, it exhibits an enhanced PCE value of 4.16%.

In order to confirm the effect of pyridine additive on the J_{sc} value of the P-t*N*p-P′:PC$_{71}$BMbased solar cell, the IPCE response of the device with active layer processed from the pyridine/THF solvent mixture was recorded. As shown in Figure3b, the device with the pyridine modified active layer (red-color line) exhibits a stronger and broader IPCE response than the solar cell with the unmodified active layer (black-color line).

The UV-vis spectra of P-t*N*p-P′:PC$_{71}$BM blend (in 1:1 weight ratio) films processed from THF with and without pyridine additive, under identical conditions, were also recorded. As shown in Figure 4, the films display almost identical absorption profiles, with the film cast from pyridine/THF mixture giving more intense absorption. This can be attributed to different film morphologies, with the P-t*N*p-P′:PC$_{70}$BM active layer blend prepared from the pyridine/THF solvent mixture having a higher degree of crystallinity.[72]

In general, the morphology of the active layer of a BHJ solar cell is critical for its performance, as it affects all processes occurring in the device, such as exciton diffusion, charge separation, charge transport and charge recombination. Ideally, the donor and acceptor components in the active layer blend should form an interpenetrating network that possesses not only enough D-A interfaces for efficient charge separation, but also continuous percolation pathways for charge transport, with the ideal BHJ donor-acceptor domain size being within the 10-20 nm range.[66, 73-76]

In order to investigate the effect of pyridine as solvent additive on the morphology of the P-t*N*p-P′:PC$_{71}$BM active layer, atomic force microscopy (AFM) images of thin films of the P-t*N*p-P′:PC$_{71}$BM blend processed from THF with and without pyridine additive (Figure 5) were obtained. The AFM image of the film processed from neat THF exhibits large phase separation domains in the range of 100-150 nm, with the root mean surface roughness being equal to 3.46 nm. However, the corresponding image of the P-t*N*p-P′:PC$_{71}$BM blend film processed from 3% v/v mixture of pyridine in THF is smoother with much smaller phase separation domains in the range of 10-20 nm and the root mean surface roughness being equal to ~1.85 nm. These results suggest a better miscibility of P-t*N*p-P′ with PC$_{71}$BM on pyridine, lead to a fine interpenetrating network. Therefore, the solar cell with the pyridine modified active layer displays more appropriate morphological features for efficient exciton dissociation and charge transport that result in enhanced J_{sc} and *FF* values.[67, 77]

The different morphology the pyridine modified P-t*N*p-P′:PC$_{71}$BM active layer blend was further investigated by X-ray diffraction (XRD) experiments. The XRD patterns of P-t*N*p-P′:PC$_{71}$BM blend thin films processed with and without pyridine additive are shown in Figure 6. The blend film processed from the pyridine/THF mixture shows a sharp diffraction peak at $2\theta = 7.34°$, whereas the blend film processed from neat THF shows a broad diffraction peak. The increase in the crystallinity may be attributed to the slow evaporation rate during the film formation with the pyridine additive. The more distinct diffraction peak of the former film suggests a higher degree of crystallinity, which in turn results in more efficient electron and hole transport.

The mobility of holes and electrons in the active layer of a BHJ solar cell are of great importance, since they affect the charge transport process and, therefore, the photocurrent generation. To explore the influence of pyridine as solvent additive on the charge transport within the active layer of the BHJ devices, the hole-only and electron-only devices were fabricated using active layers, which were processed from THF with and without pyridine additive. The mobilities of electrons and holes were estimated by modeling the dark current-voltage (*J-V*) characteristics of the hole-only and electron-only devices (shown in Figure 7a and 7b, respectively), using the space charge limited current (SCLC) method.[78] The hole mobility (μ_h) and electron mobility (μ_e) values are estimated to be 3.48×10^{-6} and 2.34×10^{-4} cm^2/Vs, respectively, for the devices fabricated from neat THF, whereas the corresponding values of μ_h and μ_e for the devices processed from 3% v/v mixture of pyridine in THF were estimated to be 2.63×10^{-5} and 2.28×10^{-4} cm^2/Vs, respectively. Apparently, the incorporation of pyridine as solvent additive significantly improves the hole mobility, but slightly decreases the electron mobility. The enhanced hole mobility can be attributed to the higher crystallinity of the pyridine modified P-t*N*p-P′:$PC_{71}BM$ active layer blend, which has been proved by UV-vis absorption spectra and XRD data of the corresponding thin film. For efficient BHJ organic solar cells, the electron mobility/hole mobility (μ_e/μ_h) ratio should be as low as possible, so that the charge transport should be balanced (unity, for an ideal organic solar cell). For the THF and pyridine/THF processed active layers, the μ_e/μ_h ratios were found to be 67.24 to 8.67, respectively. The smaller μ_e/μ_h ratio of the latter device implies a higher charge balance, which in turn results in more efficient charge transport, and it is an additional reason for the enhanced J_{sc} and PCE values of the pyridine modified device.

Conclusions

In summary, herein we present the results of our studies by using an unsymmetrical, triazine-bridged porphyrin dyad (P-t*N*p-P′) having the D-A-D molecular architecture as electron donor, in combination with $PC_{71}BM$ as electron acceptor, for the fabrication of solution-processed BHJ organic solar cells. UV-vis absorption and photoluminescence spectra of P-t*N*p-P′ and $PC_{71}BM$ blend films together with electrochemical measurements of P-t*N*p-P’ indicate that the dyad can effectively harvest photons and act as electron donor to $PC_{71}BM$ molecules. The BHJ organic solar cell based on P-t*N*p-P′:$PC_{71}BM$active layer blend in 1:1 weight ratio cast from THF resulted in a PCE value of 2.91%. However, processing the active layer blend from a 3% v/v mixture of pyridine in THF resulted in an increase of the overall photovoltaic efficiency to 4.16%. The enhanced PCE value for the device with pyridine additive is ascribed to an increase of the J_{sc} and *FF* values of the solar cell. As shown by AFM and XRD measurements, incorporation of small quantities of pyridine additive in the active layer leads to a higher degree of crystallinity. The morphological features of the modified active layer, with the smoother surface, the finer interpenetrating network and the small domain sizes in the range between 10-20 nm, lead to more efficient exciton dissociation and more balanced charge transport.

These results demonstrate that triazine-bridged porphyrin assemblies are very promising electron donors for solution-processed BHJ organic solar cells and that the utilization of proper solvent additives in their active layer, such as pyridine, can significantly enhance their photovoltaic performance.

Acknowledgements

Financial support from the European Commission (FP7-REGPOT-2008-1, Project BIOSOLENUTI No 229927), is greatly acknowledged. This research has been also co-financed by the European Union (European Social Fund–ESF) and Greek national funds through the Operational Program "Education and Lifelong Learning" of the National Strategic Reference Framework (NSRF)-Research Funding Program: Heraklitos II and Operational Program "Education and Lifelong Learning" of the National Strategic Reference Framework (NSRF) - Research Funding Program: THALIS-UOA-MIS 377252. Finally Special Research Account of the University of Crete is also acknowledged.

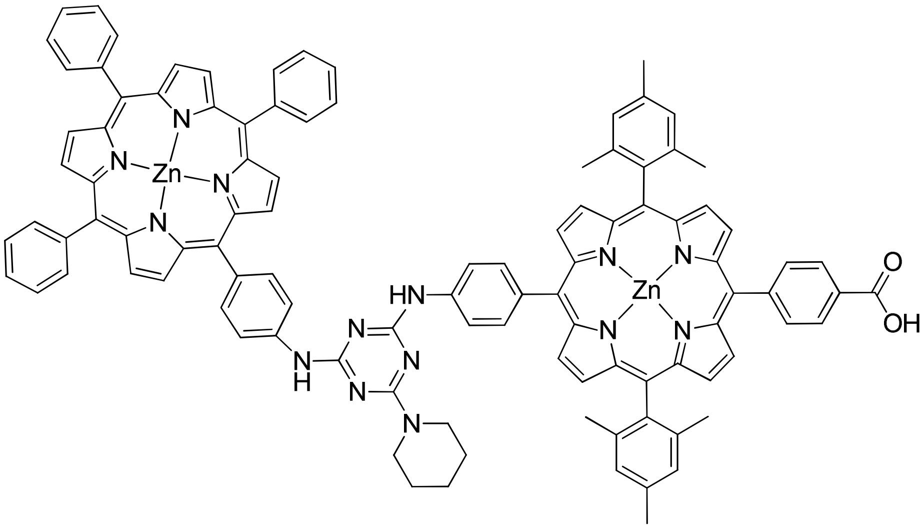

Scheme 1. Chemical structure of triazine-bridged, porphyrin dyad P-t*N*p-P′.

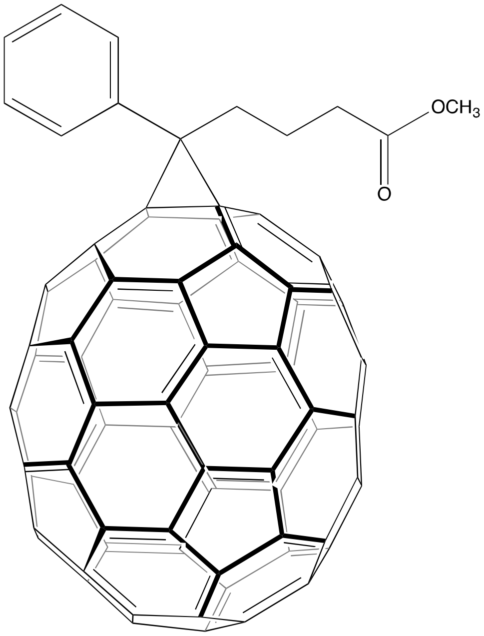

Scheme 2. Chemical structure of PC$_{71}$BM.

Table 1. Photovoltaic parameters of the BHJ organic solar cells based on differently processed active layers of P-t*N*p-P′:$PC_{71}BM$ in 1:1 weight ratio.

Active layer	J_{sc}(mA/cm^2)	V_{oc} (V)	FF	PCE (%)
P-t*N*p-P′:$PC_{71}BM$ processed from THF	6.75	0.98	0.44	2.91
P-t*N*p-P′:$PC_{71}BM$ processed from 3% v/v pyridine in THF	8.52	0.94	0.52	4.16

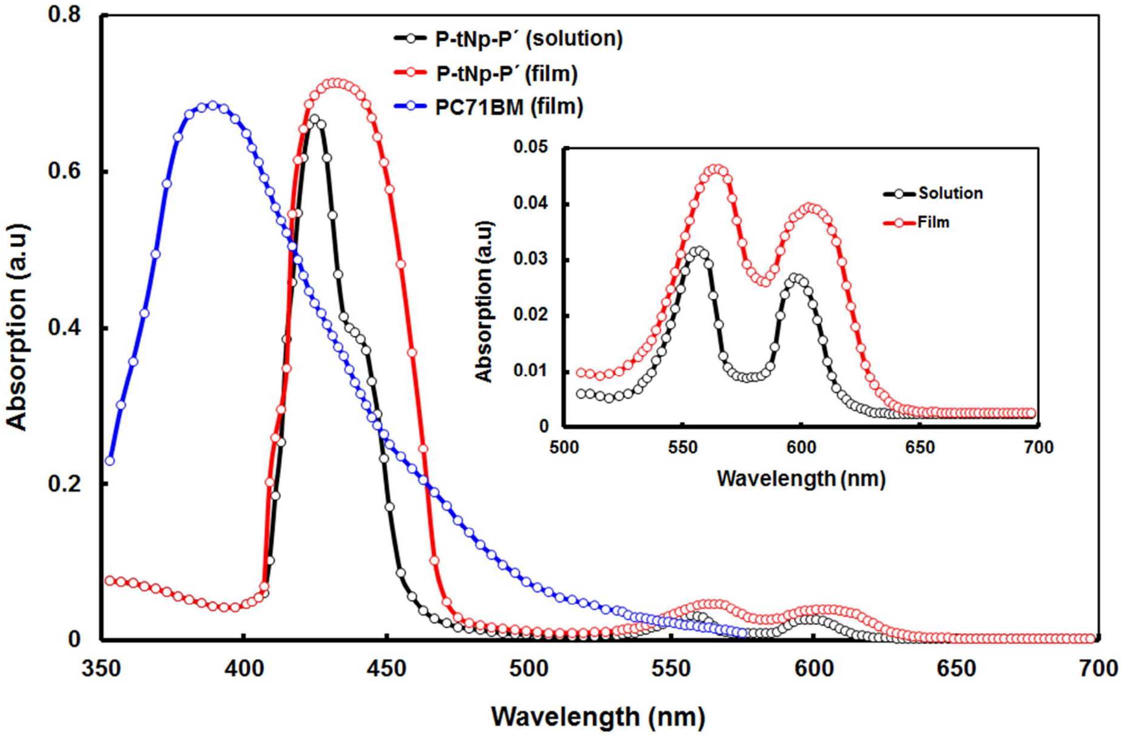

Figure 1. UV-vis absorption spectra of P-t*N*p-P´ in THF solution (black-color line) and thin film (red-color line), and $PC_{71}BM$ thin film (blue-color line).

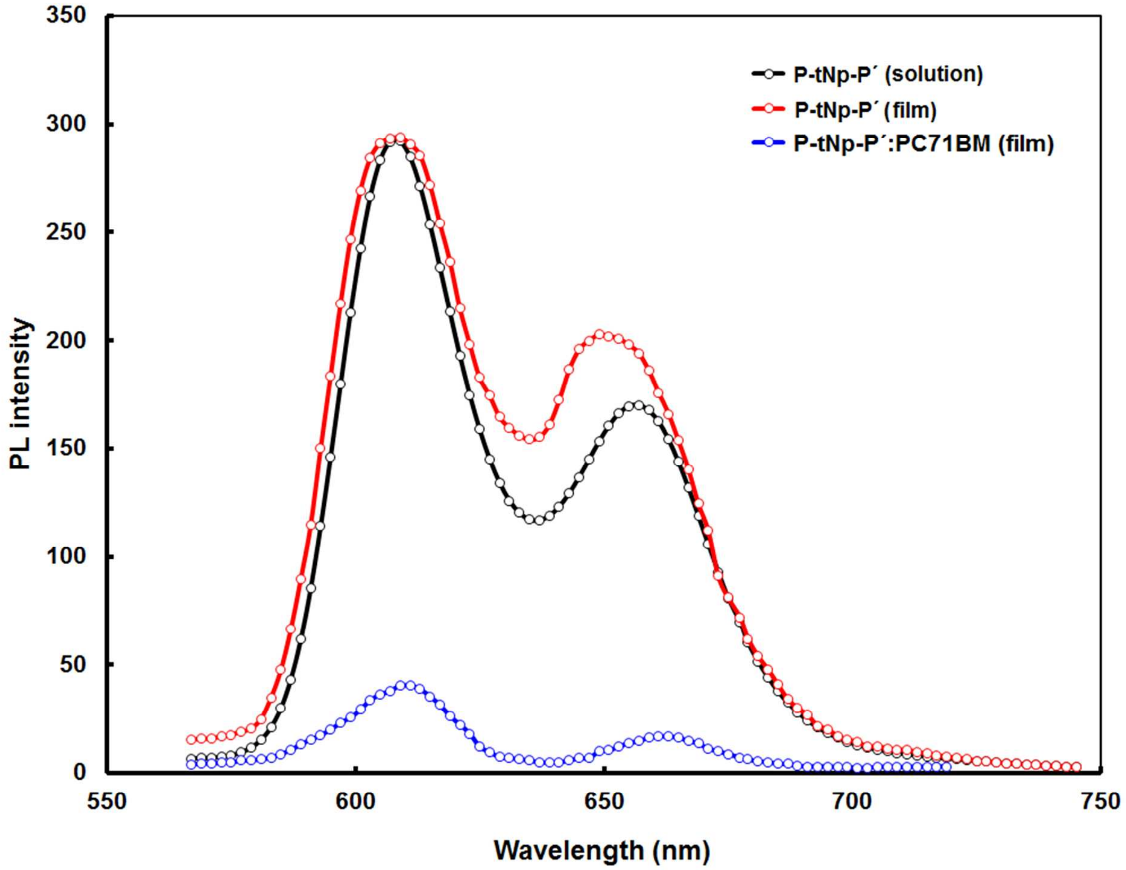

Figure 2. Isoabsorbing photoluminescence (PL) spectra of P-t*N*p-P´ in THF solution (black-color line),P-t*N*p-P´ on thin film (red-color line) and P-t*N*p-P´:PC$_{71}$BM (1:1) blend on thin film (blue-color line) processed form THF.

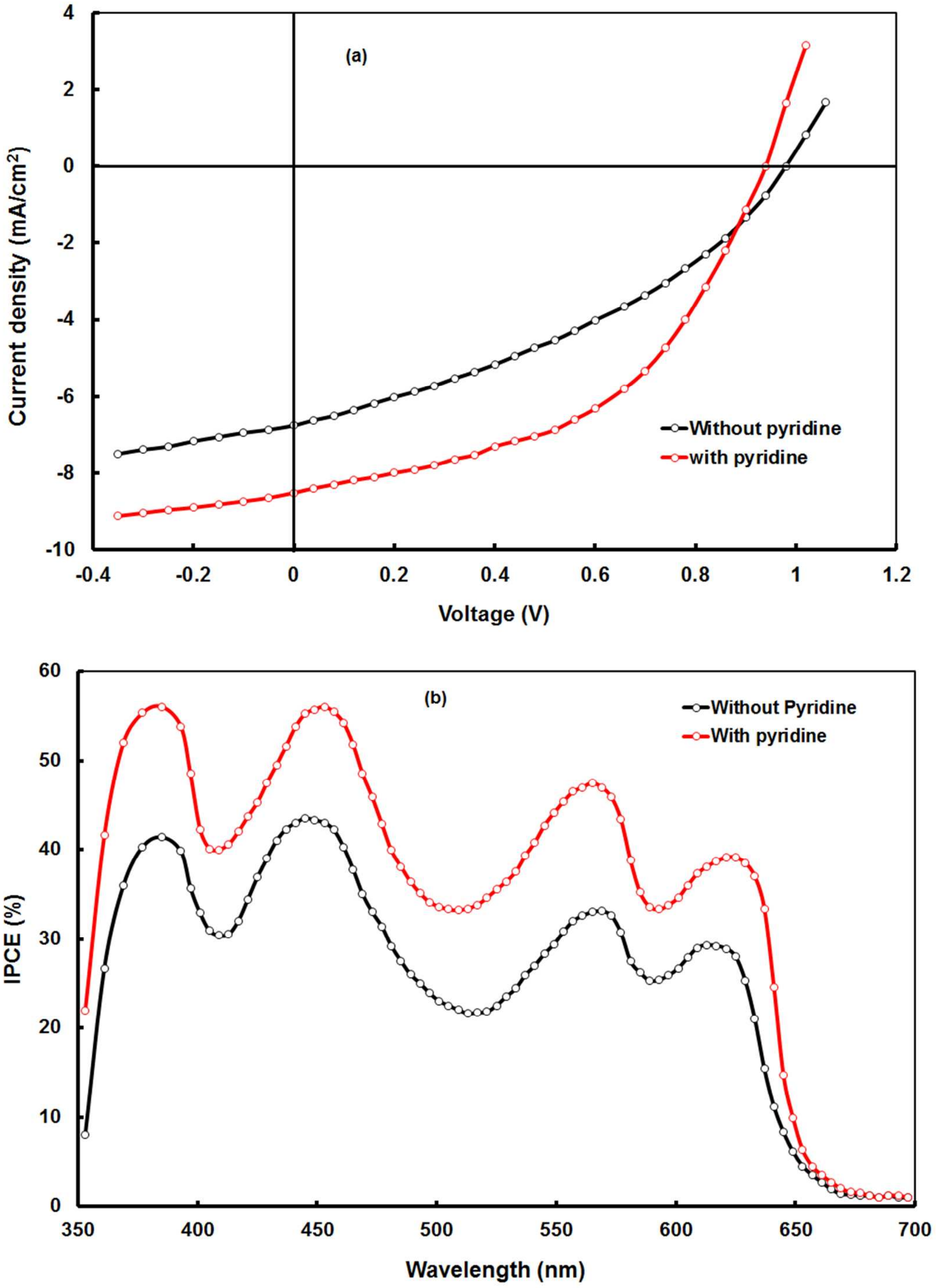

Figure 3. (a) Current-voltage (*J-V*) characteristics, and (b) IPCE spectra of BHJ organic solar cells based on active layers of P-t*N*p-P′:PC$_{71}$BM (1:1) blends processed from THF (black-color line) and 3% v/v mixture of pyridine in THF (red-color line).

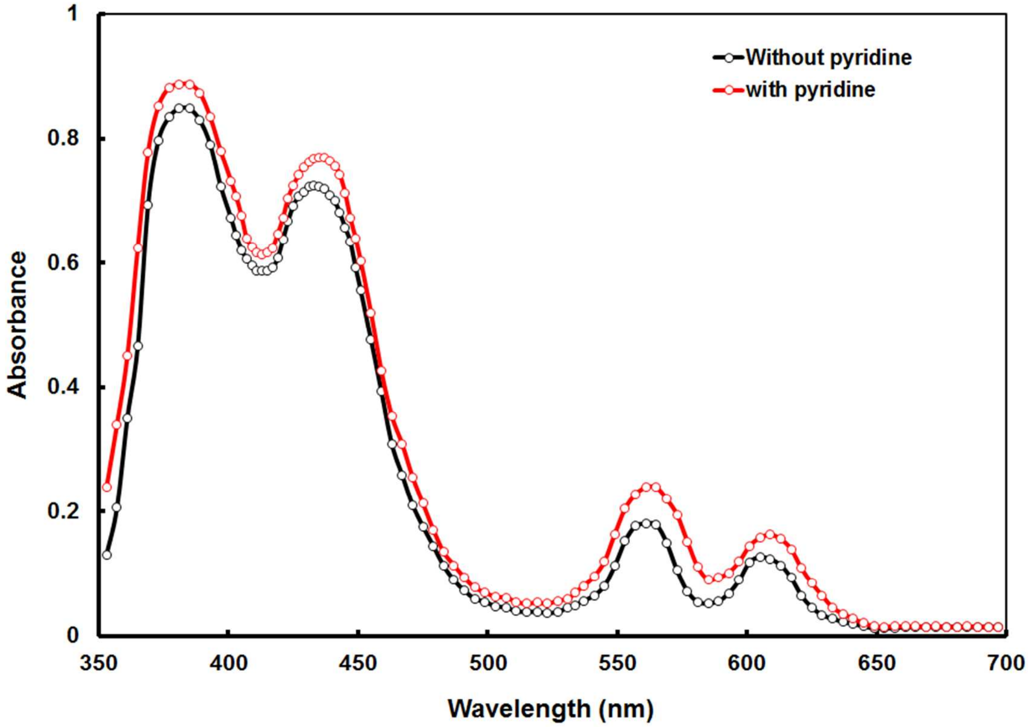

Figure 4. UV-vis absorption spectra of P-t*N*p-P′:PC$_{71}$BM (1:1) blend thin films processed from THF (black-color line) and 3% v/v mixture of pyridine in THF (black-color line).

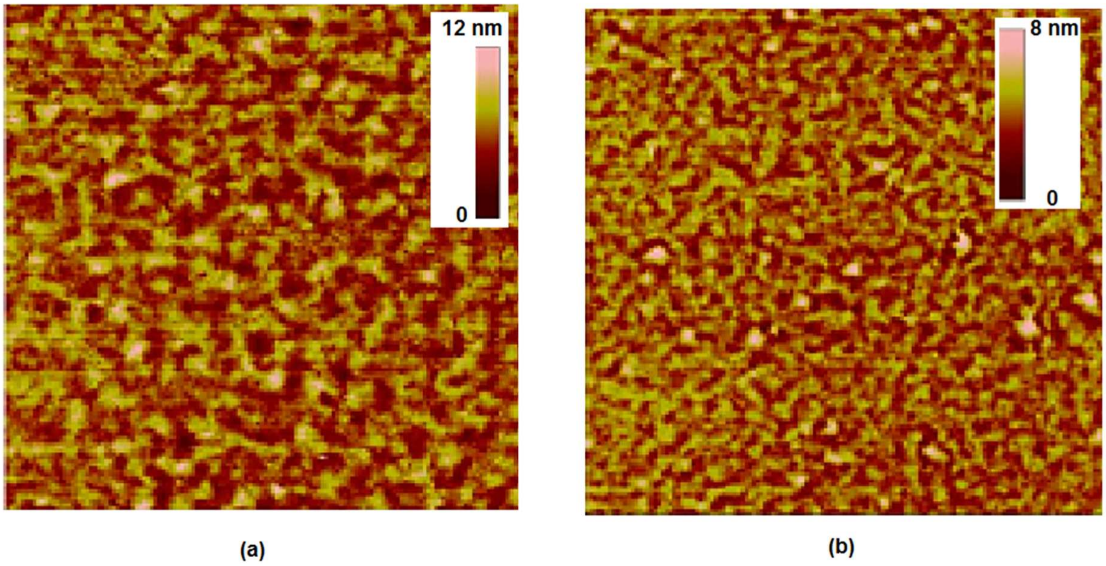

Figure 5. AFM tapping mode images (5μm×5μm) of P-t*N*p-P′:PC$_{71}$BM (1:1) blend thin films processed from (a) THF and (b) 3% v/v mixture of pyridine in THF.

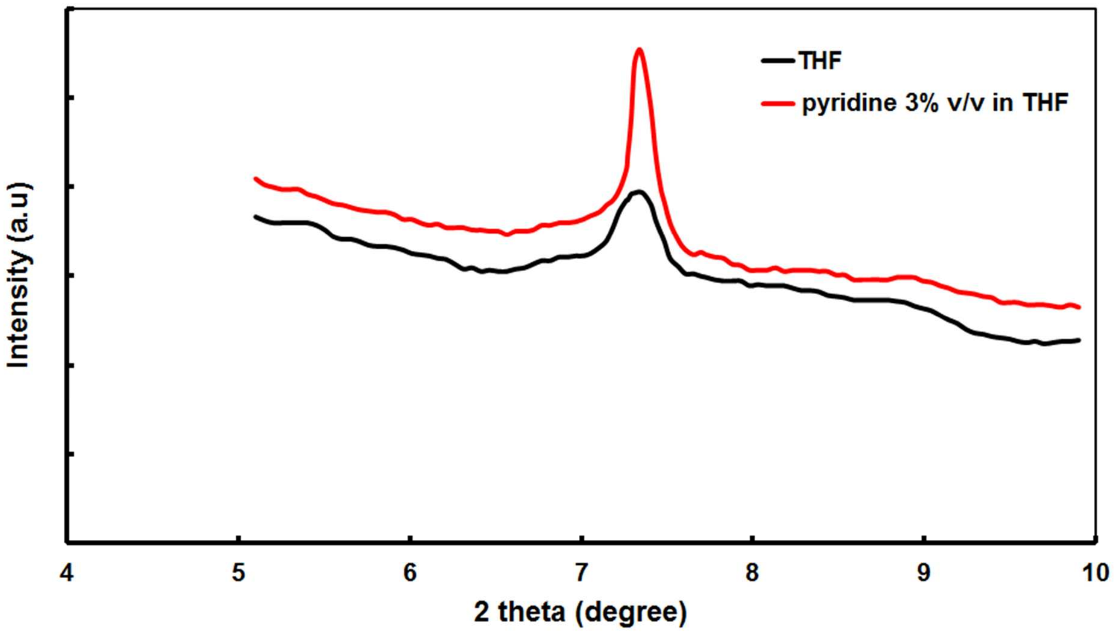

Figure 6. X-ray diffraction (XRD) patterns of P-t*N*p-P′:PC$_{71}$BM blend thin films deposited on quartz substrates processed from THF (black-color line) and 3% v/v mixture of pyridine in THF (red-color line).

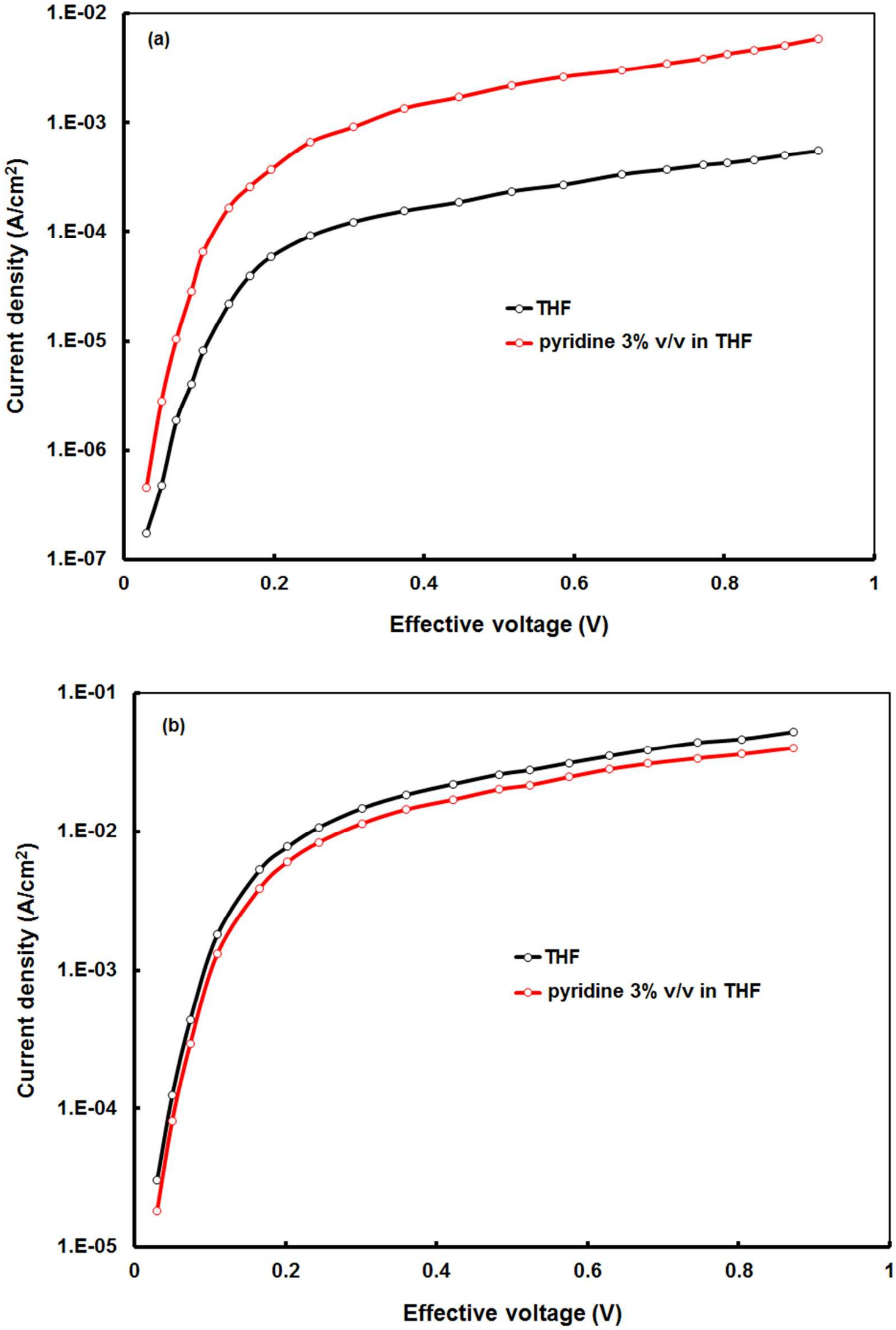

Figure 7. Current-voltage (*J*−*V*) characteristics in dark for (a) hole-only and (b) electron-only solar cell devices, using P-t*N*p-P′:PC$_{71}$BM active layer blends processed from THF (black-color line) and 3% v/v mixture of pyridine in THF (red-color line).

For table of contents use only

A triazine-bridged porphyrindyad as electron donor for solution-processed bulk hetero-junction organic solar cells

Ganesh D. Sharma[#*], *Galateia E. Zervaki*[§], *PanagiotisAggaridis, and Athanassios G. Coutsolelos*[§]*

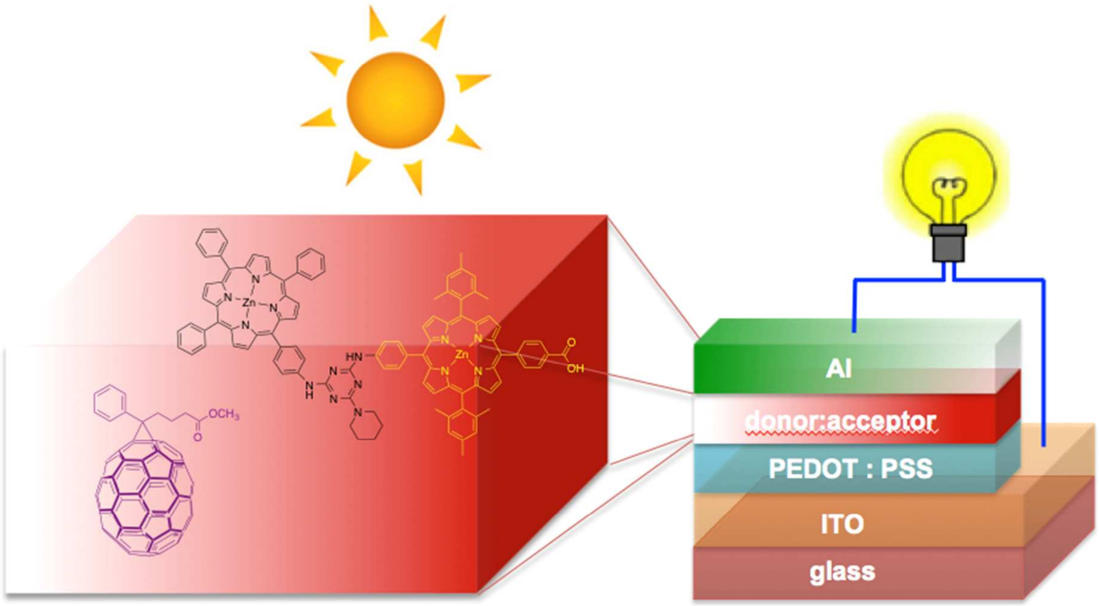

References

1. G. Yu, J. Gao, J. C. Hummelen, F. Wudl and A. J. Heeger, *Science*, 1995, **270**, 1789
2. G. Li, V. Shrotriya, J. S. Huang, Y. Yao, T. Moriarty, K. Emery and Y. Yang, *Nat. Mater.*, 2005, **4**, 864
3. S. H. Park, A. Roy, S. Beaupre, S. Cho, N. Coates, J. S. Moon, D. Moses, M. Leclerc, K. Lee and A. J. Heeger, *Nat. Photonics*, 2009, **3**, 297
4. Y. Liang, Z. Xu, J. Xia, S.-T. Tsai, Y. Wu, G. Li, C. Ray and L. Yu, *Adv. Mater.*, 2010, **22**, E135
5. S. B. Darling and F. You, *RSC Adv.*, 2013, **3**, 17633
6. N. S. Sariciftci, L. Smilowitz, A. J. Heeger, F. Wudl, *Science,* 1992,**258**, 1474
7. C. Deibel, V. Dyakonov, *Rep. Prog. Phys.,* 2010, **73**, 096401
8. K. Vakhshouri, S. V. Kesava, D. R. Kozub, E. D. Gomez, *Mater. Lett.,* 2013, **90**, 97.
9. Z. He, C. Zhong, S. Su, M. Xu, H. Wu and Y. Cao, *Nat. Photonics*, 2012, **6**, 591
10. Y. Li, *Acc. Chem. Res.*, 2012, **45**, 723
11. C. Cabanetos, A. El Labban, J. A. Barteld, J. D. Douglas, W. M. Mateker, J. M. J. Fréchet, M. D. McGhee, P. M. Beaujuge, *J. Am. Chem. Soc.*, 2013, **135**, 4656
12. S. E. Shaheen, C. J. Brabeck, N. S. Sariciftci, F. Padinger, T. Fromherz, J. C. Hummelen, *Appl. Phys. Lett.,* 2001, **78**, 841.
13. M. A. Green, K. Emery, Y. Hishikawa, W. Warta, E. D. Dunlop, *Prog.Photovolt. Res. Appl.,* 2012, **20**, 12.
14. M. P. Nikiforov, B. Lai, W. Chen, S. Chen, R. D. Schaller, J. Strzalka, J. Maser and S. B. Darling, *Energy Environ. Sci.*, 2013, **6**, 1513
15. Y. Lin, Y. Li, X. Zhan, *Chem. Soc. Rev.*, 2012, **41**, 4245
16. A. Mishra, P. Bauerle, *Angew. Chem., Int. Ed.*, 2012, **51**, 2020
17. B. Walker, C. Kim, T.-Q. Nguyen, *Chem. Mater.*, 2011, **23**, 470

18. Y. Chen, X. Wan, G. Long, *Acc. Chem. Res.*, 2013, **46**, 2645.

19. Y. Sun, G. C. Welch, W. L. Leong, C. J. Takacs, G. C. Bazan, A. J. Heeger, *Nat. Mater.,* 2012, **11**, 44

20. J. E. Coughlin, Z. B. Henson, G. C. Welch, G. Bazan, *Acc. Chem. Res.*, 2014, **47**, 257

21. J. Zhou, Y. Zuo, X. Wan, G. Long, Q. Zhang, W. Ni, Y. Liu, Z. Li, G. He, C. Li, B. Kan, M. Li, Y. Chen, *J. Am. Chem. Soc.*, 2013, **135**, 8484

22. S. Shen, P. Jiang, C. He, J. Zhang, P. Shen, Y. Zhang, Y. Yi, Z. Zhang, Z. Li, Y. Li, *Chem. Mater.*, 2013, **25**, 2274.

23. T. S. van der Poll, J. A. Love, N. Thuc-Quyen and G. C. Bazan, *Adv. Mater.*, 2012, **24**, 3646

24. V. Gupta, A. K. K. Kyaw, D. H. Wang, S. Chand, G. C. Bazan and A. J. Heeger, *Sci. Rep.*, 2013, **3**, 1965

25. http://www.heliatek.com/newscenter/latest_news/neuer-weltrekord-fur-organische-solarzellen-heliatek-behauptet-sich-mit-12-zelleffizienz-als-technologiefuhrer/?lang=en "Small molecule organic solar cells by Heliatek/IAPP with a certified efficiency of 12.0%", press release, January 2013; http://www.heliatek.com (accessed February 2013)

26. M. J. Gouterman, *Mol. Spectrosc.,*1961, **6**, 138.

27. R. B. Ambre, G.-F. Chang, M. R. Zanwar, C.-F. Yao, E. W.-G. Diau and C.-H. Hung *Chem. Asian J.*, 2013, **8**, 2144

28. T. Bessho, S. M. Zakeeruddin, C.-Y. Yeh, E. W.-G. Diau, M. Grätzel, *Angew. Chem. Int. Ed.*, 2010, **49**, 6646

29. J. Lu, X. Xu, Z. Li, K. Cao, J. Cui, Y. Zhang, Y. Shen, Y. Li, J. Zhu, S. Dai, W. Chen, Y. Cheng, M. Wang, *Chem. Asian J.*, 2013, **8**, 956

30. C. Yi, F. Giordano, N.-L. Cevey-Ha, H. N. Tsao, S. M. Zakeeruddin and M. Grätzel, *ChemSusChem*, 2014, **7**, 1107

31. M. J. Griffith, K. Sunahara, P. Wagner, K. Wagner, G. G. Wallace, D. L. Officer, A. Furube, R. Katoh, S. Mori, A. J. Mozer, *Chem. Commun.*, 2012, **48**, 4145

32. A. Yella, H. W. Lee, H. N. Tsao, C. Yi, A. K. Chandiran, M. K. Nazeeruddin, E. W. G. Diau, S. M. Zakeeruddin, M. Grätzel, *Science*, 2011, **334**, 629

33. S. Mathew, A. Yella, P. Gao, R. Humphry-Baker, B. F.E. Curchod, N. Ashari-Astani, I. Tavernelli, U. Rothlisberger, Md. K. Nazeeruddin and M. Grätzel, *Nature Chemistry*, 2014, **6**, 242.

34. Q. Sun, L. Dai, X. Zhou, L. Li, Q. Li, *Appl. Phys. Lett.*, 2007, **91**, 253505/1

35. T. Oku, T. Noma, A. Suzuki, K. Kikuchi, S. Kikuchi, *J. Phys. Chem. Solids*, 2010, **71**, 551

36. M. V. Martinez-Diaz, G. de la Torrea and T. Torres, *Chem. Commun.*, 2010, **46**, 7090

37. M. G. Walter, A. B. Rudine and C. C. Wamser, *J. Porphyrins Phthalocyanines*, 2010, **14**, 759

38. T. Hasobe, H. Imahori, P. V. Kamat, T. K. Ahn, S. K. Kim, D. Kim, A. Fujimoto, T. Hirakawa and S. Fukuzumi, *J. Am. Chem. Soc.*, 2005, **127**, 1216

39. Hatano, N. Obata, S. Yamaguchi, T. Yasuda, Y. Matsuo, *J. Mater. Chem.*, 2012, **22**, 19258.

40. Y. Huang, L. Li, X. Peng, J. Peng, Y. Cao, *J. Mater. Chem.*, 2012, **22**, 21841

41. L. Li, Y. Huang, J. Peng, Y. Cao, X. Peng, *J. Mater. Chem. A*, 2013, **1**, 2144

42. H. Qin, L. Li, F. Guo, S. Su, J. Peng, Y. Cao and X. Peng, *Energy Environ. Sci.*, 2014, **7**, 1397

43. G. D. Sharma, D. Daphnomili, S. Biswas, A. G. Coutsolelos, *Org. Electron.*, 2013, **14**, 1811

44. P. A. Angaridis, T. Lazarides, A. G. Coutsolelos, *Polyhedron*, 2014, DOI:10.1016/j.poly.2014.04.039

45. G. E. Zervaki, M. S. Roy, M. K. Panda, P. A. Angaridis, A. G. Coutsolelos, G. D. Sharma, *Inorg. Chem.*, 2013, **53**, 9813

46. G. E. Zervaki, P. A. Angaridis, E. N. Koukaras, G. D. Sharma, A. G. Coutsolelos, Inorg. Chem. Front., 2014, **1**, 25

47. G. D. Sharma, G. E. Zervaki, P. A. Angaridis, T. N. Kitsopoulos, and A. G. Coutsolelos, *J. Phys. Chem. C*, 2014, **118**, 5968

48. R. Fink, C. Frenz, M. Thelakkat and H. Schmidt, *Macromolecules*, 1997, **30**, 8177

49. R. Fink, Y. Heischkel, M. Thelakkat and H. Schmidt, *Chem. Mater.*, 1998, **10**, 3620

50. J. Kang, D. Lee, H. Park, Y. Park, J. W. Kim, W. Jeong, K. Yoo, K. Go, S. Kim and J. Kim, *J. Mater. Chem.*, 2007, **17**, 3714

51. A. Richard, H. A. Klenklera, A. Tranc, D. Z. Popovic and G. Xu, *Org. Electron.*, 2008, **9**, 285

52. H. Zhong, E. Xu, D. Zeng, J. Du, J. Sun, S. Ren, B. Jiang and Q. Fang, *Org. Lett.*, 2008, **10**, 709

53. T. Hasobe, A. S. D. Sandanayaka, T. Wada and Y. Araki, *Chem. Commun.*, 2008, 3372

54. Y. Matsuo, Y. Sato, T. Niinomi, I. Soga, H. Tanaka and E. Nakamura, *J. Am. Chem. Soc.*, 2009, **131**, 1127

55. A. Luechai, J. Gasiorowski, A. Petsom, H. Neugebauer, N. S. Sariciftci and P. Thamyongkit, *J. Mater. Chem.*, 2012, **22**, 23030

56. G. E. Zervaki, P. A. Angaridis, E. N. Koukaras, G. D. Sharma and A. G. Coutsolelos, *Inorg. Chem. Front.*, 2014, **1**, 256

57. K. Ladomenou, T. Lazarides, M. K. Panda, G. Charalambidis, D. Daphnomili, A. G. Coutsolelos, *Inorg. Chem.,* 2012, **51**, 10548.

58. T. Hasobe, P. V. Kamat, M. A. Absalom, Y. Kashiwagi, J. Sly, M. J. Crossley, K. Hosomizu, H. Imahori and S. Fukuzumi, *J. Phys. Chem. B*, 2004, **108**, 12865

59. T. Umeyama, T. Takamatsu, N. Tezuka, Y. Matano, Y. Araki, T. Wada, O. Yoshikawa, T. Sagawa, S. Yoshikawa and H. Imahori, *J. Phys. Chem. B*, 2011, **113**, 10798

60. C.-L. Wang, W.-B. Zhang, C.-H. Hsu, H.-J. Sun, R. M. V. Horn, Y. Tu, D. V. Anokhin, D. A. Ivanov and S. Z. D. Cheng, *Soft Matter*, 2011, **7**, 6135

61. W. Ma, C. Yang, X. Gong, K. Lee, A. J. Heeger, *Adv. Funct. Mater.*, 2005, **15**, 1617

62. J. A. Mikroyannidis, A. N. Kabanakis, S. S. Sharma, G. D. Sharma, *Adv. Funct. Mater.*, 2011, **21**, 746.

63. Y. Zhao, Z. Xie, Y. Qu, Y. Geng, L. Wang, *Appl. Phys. Lett.*, 2007, **90**, 043504/1

64. G. Li, Y. Yao, H. Yang, V. Shrotriya, G. Yang, Y. Yang, *Adv. Funct. Mater.*, 2007, **17**, 1636

65. G. D. Sharma, P. Suresh, S. S. Sharma, Y. K. Vijay, J. A. Mikroyannidis, *ACS Appl. Mater. Interfaces,* 2010, **2**, 504.

66. J. Peet, J. Y. Kim, N. E. Coates, W. L. Ma, D. Moses, A. J. Heeger, G. C. Bazan, *Nat. Mater.,* 2007, **6**, 497

67. M. S. Su, C. Y. Kuo, M. C. Yuan, U. S. Jeng, C. J. Su, K. H. Wei, *Adv. Mater.,* 2011, **23**, 3315

68. A. Tamayo, T. Kent, M. Tantitiwat, M. A. Dante, J. Rogeres, T. Q. Nguyen, *Energy Environ. Sci.,* 2009, **2**, 1180

69. H. Fan, H. Shang, Y. Li, X. Zhang, *Appl. Phys. Lett.,* 2010, **97**, 133302

70. B. Walker, C. Kim, T. Q. Nguyen, *Chem. Mater.,* 2010, **23**, 470

71. M. L. Keshtov, D. V. Marochkin, V. S. Kochurov, A. R. Khokhlov, E. N. Koukaras, G. D. Sharma, *Polym. Chem.*, 2013, **4**, 4033.

72. F.-C. Chen, H.-C. Tseng and C.-J. Ko, *Appl. Phys. Lett.*, 2008, **92**, 103316

73. B. C. Thompson, J. M. J. Frechet, *Angew. Chem. Int. Ed.*, 2008, **47**, 58

74. A. J. Heeger, *Adv. Mater.*, 2014, **26**, 10

75. M. T. Dang , L. Hirsch , G. Wantz , J. D. Wuest, *Chem. Rev.*, 2013, **113**, 3734

76. J. K. Lee, W. L. Ma, C. J. Brabec, J. Yuen, J. S. Moon, J. Y. Kim, K. Lee, G. C. Bazan, A. J. Heeger, *J. Am. Chem. Soc.*, 2008, **130**, 3619.

77. C. H. Woo, P. M. Beaujuge, T. W. Holcombe, O. P. Lee and J. M. J. Frechet, *J. Am. Chem. Soc.*, 2010, **132**, 15547.

78. P. W. M. Blom, M. J. M. deJong and M. G. vanMunster, *Phys. Rev. B: Condens. Matter*, 1997, **55**, R656.